

# An Analysis of Multipath Mitigation Techniques suitable for Geodetic Antennas

Robin Granger, *Roke Manor Research Ltd*  
Dr Steve Simpson, *Roke Manor Research Ltd*

## BIOGRAPHY

### Robin Granger MEng

Robin graduated from Southampton University in 1999 with a Masters Degree with Distinction in Electronic Engineering, and now works at Roke Manor Research Ltd where he is a Consultant Engineer in the Electromagnetic Engineering Technology Centre. His work on antennas and electromagnetics includes designing a multiband Planar Inverted 'F' Antenna for the Siemens CX75 mobile phone and a 4.25Gbit/s non-contact rotary data link for Siemens Medical Solutions.

### Stephen HW Simpson BSc, PhD

Steve Simpson graduated from the university of Salford with first class honours in electronics in 1974 and went on to post graduate studies in microwave scattering at the university of Sheffield, from where he obtained his PhD in 1979. He spent a short time at British Aerospace (Dynamics) before moving to Roke Manor Research Ltd in July 1979. Steve has held a wide variety of posts at Roke, including Group Leader positions in: Air Traffic Management and Navigation, Computational Electromagnetics and Electromagnetic Engineering, which is his current position.

## ABSTRACT

Roke Manor Research has been actively involved in the development of a geodetic-grade receiver and antenna for Galileo under the "Advanced Receiver Terminal for User Services" (ARTUS) programme, supported by the European GNSS Supervisory Authority (GSA).

A paper [1] was presented by Roke at ION GNSS 2006 (and was subsequently featured in GPS World magazine, Feb 2007) which described the development of a wide bandwidth antenna with good axial ratio and phase centre stability ideally suited to geodetic and precise positioning applications requiring multiple GNSS carriers. Whilst bandwidth and phase centre stability are important performance criteria, the antenna must also reject multipath; another major source of phase error.

In this paper, we present an analysis of the multipath environment in perhaps the most demanding of

applications, namely the GNSS Reference Station. It is assumed that reference station antennas are generally sited well clear of buildings, trees and other obstructions and so attention need only be paid to multipath originating from the surface immediately below the antenna. We explain how multipath interacts with the antenna, through the processes of diffraction and surface wave propagation, and how a local groundplane can improve the situation. We also show that the traditional approximation of the ground as an infinite, perfectly conducting smooth planar surface does not apply in many real-world situations. For example, ground moisture content and surface roughness can have a significant impact on multipath.

Using proprietary simulation tools it is possible to predict the likely multipath errors for any particular antenna, groundplane and ground surface combination using antenna pattern data derived either from simulations or anechoic chamber measurements. The paper will describe how such simulations may be performed.

Finally, we propose a number of techniques which may be useful in reducing the effects of multipath from the ground. Some of these, such as the choke ring groundplane, are well-known; others presented perhaps for the first time. In particular, a novel, broadband groundplane structure is described which is suitable for multi-GNSS reference station installations. This groundplane, when combined with the ARTUS antenna, has been shown in simulations to reject multipath by 20dB or more at all Galileo and GPS carriers, and with scope for further improvements.

## INTRODUCTION

Multipath is the propagation phenomenon whereby signals reach the receiver via a number of different propagation paths. In the specific case of GNSS positioning, the dominant multipath mechanisms are reflection and diffraction from the ground and other nearby structures, e.g. buildings, vegetation or vehicles. This type of multipath is, for GPS, one of the most significant causes of pseudorange errors.

Typically, multipath manifests itself in the received signal as a number of attenuated, phase-shifted and delayed (since the indirect path is always longer) replicas of the line-of-sight (LOS) signal summed together. When the multipath delay is large, a receiver can readily resolve the multipath and will not suffer significant effects on performance. Shorter delays, from grazing reflections and close-in structures, distort the correlation function between the received signal and locally-generated reference signal, introducing errors in pseudorange measurements. In both cases, crucially, carrier phase is also modified.

In the scope of this paper, where the application is a static reference station receiver, one would expect the environment surrounding the station to be reasonably free of large buildings, vegetation, etc. which might result in multipath of the former kind (long delays). One would also expect the absolute location of the antenna reference point (ARP) to be known very accurately, so it is assumed here that pseudorange estimates are free of error to at least the nearest symbol, if not the nearest whole carrier cycle. Thus the remaining problem is to minimise or compensate for the carrier phase error due to close-in reflections from the ground beneath the antenna.

It is worth noting that this can only be done by:

- careful antenna design, the use of choke rings, absorbing material or a local ground plane, or by modifying the materials and/or surface shape of the ground beneath the antenna; or by
- characterising the antenna and its installation to enable corrections to be made in the receiver.

## CHARACTERISATION OF MULTIPATH

In this section, we discuss methods for modelling and predicting multipath effects, and derive acceptable limits for a given position accuracy.

Figure 1 illustrates the so-called ‘two-ray’ reflection model, where multipath is produced by a single, specular reflection from the ground beneath the antenna. The ground is assumed to be infinitely large (so there are no edge effects), perfectly smooth (i.e. only specular reflection) and composed of a homogeneous dielectric medium with complex relative permittivity  $\epsilon_r$ . The antenna is placed above the ground by some distance,  $h$ , and is illuminated with a right-hand circularly-polarised (RHCP) plane wave arriving at angle  $\theta$ . The antenna is typically characterised by its magnitude and phase response, in two orthogonal polarisations, at every angle of incidence (this is denoted  $\hat{C}$  later on). In this simple axially-symmetric scenario, a two-dimensional model is

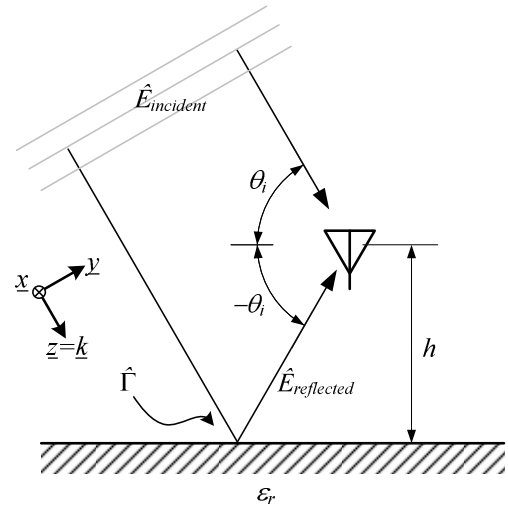


**Figure 1. The two-ray reflection model**

sufficient, so the antenna need only be represented along a single elevation cut, but a real antenna is likely to have some azimuth dependence; in other words  $\hat{C}$  is a function of both  $\theta$  and  $\phi$ .

The reflected wave, incident on the antenna at angle  $-\theta$  (Law of Reflection), is attenuated and depolarised due to the electric properties of the ground. In other words, the horizontal and vertical electrical components of the wave are modified, upon reflection, by different amounts, so the resulting wave is not necessarily circularly polarised and may not even be right-handed. The precise degree of depolarisation is given by the Fresnel Reflection Coefficients [2].

In the simplest case, where the reflecting surface is a Perfect Electrical Conductor (PEC), the reflected wave is not attenuated at all, and is perfectly CP, but suffers a complete reversal of ‘handedness’ – RHCP becomes LHCP. In more typical situations, where the ground is a lossy material like soil, concrete, etc., a similar effect can be seen at angles of incidence near zenith, albeit with some attenuation of the reflected signal. At progressively lower angles, however, the polarisation becomes first left-hand elliptic and then linear (at the quasi-Brewster angle) before becoming right-hand elliptic near the horizon. An example of this effect is shown in Figure 2, where right-hand polarisations are drawn with dotted lines, and left-hand with solid lines for clarity. Note that the term ‘vertical’ for the  $y$ -axis is a little misleading, since it is only truly vertical for waves propagating parallel to the ground (i.e. from the horizon). More precisely, the  $y$ -axis is tangential to the *plane of incidence*, and  $x$  is normal to it.

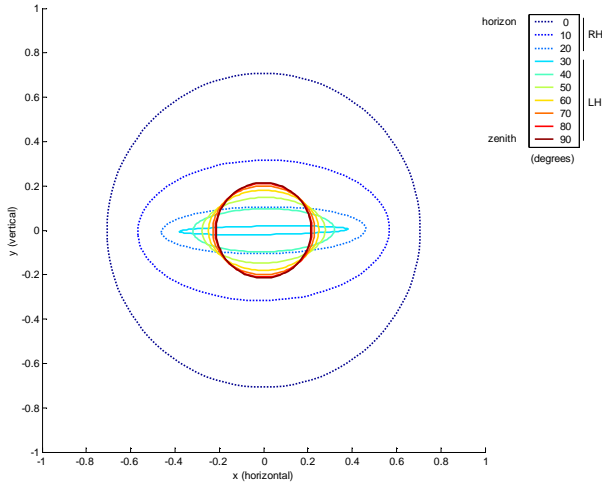


**Figure 2. Depolarisation of a Unit-Amplitude RHCP Wave by Reflection from a Dielectric Surface having Soil-like Properties ( $\kappa=3.5$ ,  $\sigma=0.0146 \text{ Sm}^{-1}$ )**

It is convenient to represent the model algebraically using Jones calculus [17], where a signal is represented by the vector

$$\hat{E} = \begin{pmatrix} E_x \\ E_y \end{pmatrix} = \begin{pmatrix} a_x e^{i\theta_x} \\ a_y e^{i\theta_y} \end{pmatrix}$$

and  $E_x$ ,  $E_y$  are the complex ‘phasor’  $\underline{x}$  and  $\underline{y}$  components of the electric field. Here we use the caret symbol ( $\hat{\cdot}$ ) for convenience to denote a Jones vector or matrix, and underlined characters to denote spatial vectors. For example, a unit amplitude wave linearly polarised in the  $\underline{x}$  direction might be given by

$$\hat{E} = \begin{pmatrix} 1 \\ 0 \end{pmatrix}$$

In another example, a unit amplitude wave which is right-hand circularly polarised might be given by

$$\hat{E} = \frac{1}{\sqrt{2}} \begin{pmatrix} 1 \\ -i \end{pmatrix}$$

Note that this representation system is only valid for polarised, coherent waves, otherwise the more unwieldy Stokes parameters must be used. In the following discussion, all signals and waves are harmonic (i.e. single frequency and time-invariant).

As explained in [2], the voltage signal (in phasor form) apparent at an antenna’s output port, in response to an incident wave, is given by the product of the wave  $\hat{E}$  and the complex conjugate transpose of the antenna response  $\hat{C}$  (also a Jones vector), in other words:

$$V = \hat{C}^* \times \hat{E} \quad (1)$$

More formally,  $\hat{C}$  represents the wave (propagating in the opposite direction) produced if the antenna were stimulated with a unit amplitude voltage signal (and this is how it may be measured for a real antenna) but for simplicity we can refer to it as the antenna’s response.

The case of an ideal RHCP antenna (with gain = 1) illuminated by a RHCP wave of unit amplitude yields a signal  $V$  where

$$V = \hat{C}_{RHCP}^* \times \hat{E}_{RHCP} = \frac{1}{\sqrt{2}} (1 \quad i) \times \frac{1}{\sqrt{2}} \begin{pmatrix} 1 \\ -i \end{pmatrix} = 1$$

as expected. If a LHCP antenna were used instead:

$$V = \hat{C}_{LHCP}^* \times \hat{E}_{RHCP} = \frac{1}{\sqrt{2}} (1 \quad -i) \times \frac{1}{\sqrt{2}} \begin{pmatrix} 1 \\ -i \end{pmatrix} = 0$$

also as expected. This demonstrates what is known as the *polarisation efficiency* of an antenna – the degree to which the antenna’s polarisation is ‘matched’ to that of the illuminating wave. In the first example, the perfect match produced a maximum response, and in the second example a perfect mismatch produced a zero response even though the antenna gain and illuminating wave was the same in each case.

Returning now to the problem of modelling single-ray multipath, the received signal (i.e. voltage at the antenna output port) is given as the sum of the direct and reflected signals, each modified by the antenna response at the corresponding angle:

$$S_{total} = S_{incident} + S_{reflected} \quad (2)$$

$$S_{incident} = \hat{C}(\theta_i)^* \hat{E}_{incident} \quad (3)$$

$$S_{reflected} = \hat{C}(-\theta_i)^* \hat{E}_{reflected} \quad (4)$$

The reflected wave is simply the incident wave depolarised by reflection, and then phase-shifted by the angle  $\delta$  to account for the additional phase rotation experienced by the indirect wave due to the extra distance.

$$\hat{E}_{reflected} = \Gamma \hat{E}_{incident} e^{j\delta} \quad (5)$$

$$\delta = \frac{4\pi h}{\lambda} \sin \theta_i \quad (6)$$

The effects of reflection from the ground are represented as a scattering matrix, of the form

$$\Gamma = \begin{pmatrix} \Gamma^{xx} & \Gamma^{xy} \\ \Gamma^{yx} & \Gamma^{yy} \end{pmatrix}$$

For a linear system where the  $\underline{x}$  and  $\underline{y}$  directions are orthogonal,  $\Gamma^{yy}$  and  $\Gamma^{yx}$  are zero and the terms  $\Gamma^{xx}$  and  $\Gamma^{xy}$  are the Fresnel Reflection Coefficients for the electric field normal ( $\underline{x}$ ) and tangential ( $\underline{y}$ ) to the plane of incidence respectively.

### MULTIPATH REJECTION REQUIREMENTS

Equations (2) to (5) can be arranged into the phasor form

$$S_{total} = S_{incident} (1 + \alpha e^{j\varphi})$$

This is obvious since  $S$ , the wanted direct signal, is corrupted simply by the addition of a single attenuated, phase-shifted version of itself – as is illustrated in Figure 3. The factors  $\alpha$  and  $\varphi$  are the combined magnitude and phase effects of the antenna pattern, the reflection from the ground and the difference in path lengths of the two rays. If we are interested in reducing the carrier phase error, we must make  $\alpha$  as small as possible and  $\varphi$  as close as possible to zero or pi – notice that  $\varphi$  is the phase *difference* between the direct and reflected signals. If it is not possible, or very difficult, to control the phase term  $\varphi$ , then the problem reduces to simply minimising  $\alpha$  – the ratio of magnitudes of the reflected and direct signals. In the general case where  $\varphi$  is unknown, clearly the largest possible phase error is  $\gamma_{max}$ , such that  $\tan(\gamma_{max}) = \alpha$ . Since carrier phase error is directly related to pseudorange error, we can then place an upper limit on  $\alpha$  for a given position accuracy.

As an example, suppose we require a carrier phase accuracy of 19 degrees, which is about 10mm range at GPS L1. Let's also suppose that no attempt is made to reduce multipath by phase cancellation, i.e. the phase is

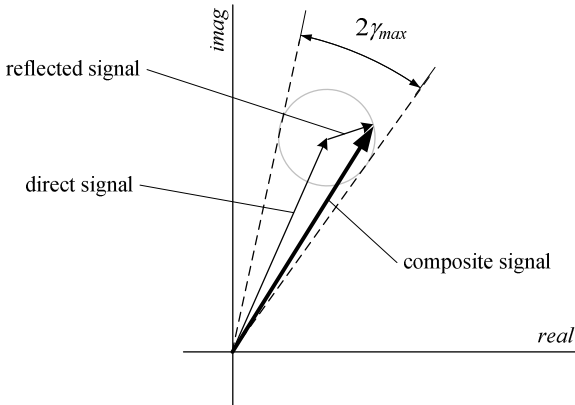


**Figure 3. Diagram representing vector summation of the direct and reflected signals**

unknown or uncontrolled. The multipath signal must therefore be no larger than  $\tan(19\text{degrees}) = 0.34$  of the magnitude of the direct signal which relates to a rejection factor of about -9.3dB.

It is possible to determine the phase difference  $\varphi$ , as well as amplitude difference  $\alpha$ , between the direct and reflected signals, if the antenna pattern (magnitude and phase), its height above the ground and the ground material parameters are known. Thus it is possible to determine, and potentially compensate for, the actual carrier phase error  $\gamma$  for a given angle of incidence rather than just the largest possible error  $\gamma_{max}$ .

In the special case of a PEC ground surface, where the amplitude of the reflected wave is not attenuated, the ratio  $\alpha$  is entirely dependent on the antenna gain pattern, given by (7). More specifically, it is the ratio of LHCP voltage response at angles below the horizon to RHCP voltage response at corresponding angles above the horizon.

$$\alpha_{PEC} = \frac{|g_{LHCP}(-\theta_i)|}{|g_{RHCP}(\theta_i)|} \quad (7)$$

Sometimes, this is crudely simplified to just the ratio of total downward gain to total upward gain, called the Down-Up Ratio [5][6], or referred to as  $G$  [14], but this can yield inaccurate results near the horizon where the 'up' and 'down' gains converge to the same value, and so their ratio becomes unity, but where the antenna may still exhibit significant polarisation rejection of the multipath.

Whichever the method, the phase error for the PEC special case is given by

$$\sin \gamma = \frac{\sin \delta}{\sqrt{\alpha^{-2} + 2\alpha^{-1} \cos \delta + 1}} \quad (8a)$$

or equivalently by

$$\gamma = \tan^{-1} \frac{\alpha \sin \delta}{1 + \alpha \cos \delta} \quad (8b)$$

For the more general scenario of a lossy dielectric ground, the rejection factor  $\alpha$  and the phase error  $\gamma$  must include the depolarisation effects of the ground making an algebraic solution considerably harder. Solving numerically, however, is straightforward using Equations (3) and (4) as follows:

$$\alpha = \frac{|S_{reflected}|}{|S_{incident}|} \quad (9)$$

and

$$\gamma = \angle(S_{incident} + S_{reflected}) - \angle S_{incident} \quad (10)$$

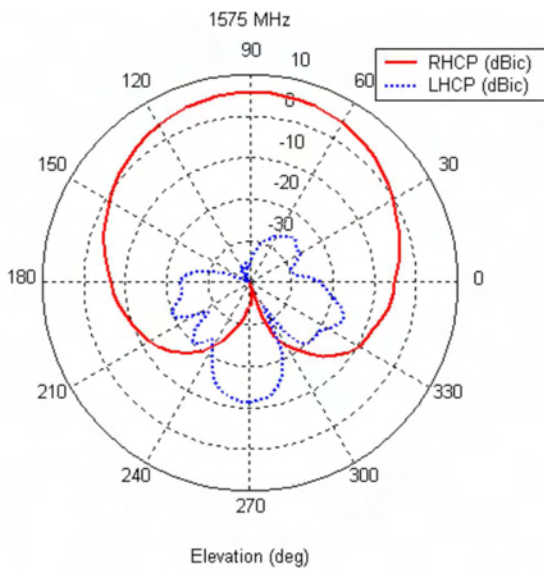


**Figure 4. RH and LHCP gain patterns for the ARTUS antenna at L1**

Note that expression (9) gives exactly the same result as (7) when the ground has the properties of a PEC. It is useful to use the PEC result to be able to compare different antennas without the complication of specifying a ‘standard’ ground material.

#### MULTIPATH PERFORMANCE FOR THE ARTUS ANTENNA

As an example, we shall consider the wideband geodetic antenna developed under the ARTUS programme and the object of the last ION GNSS paper [1]. It was measured in an anechoic chamber in order to determine  $\hat{C}$ : the magnitude and phase response in two orthogonal polarisations for a range of elevation angles and at a variety of frequencies within the GNSS bands. Figure 4

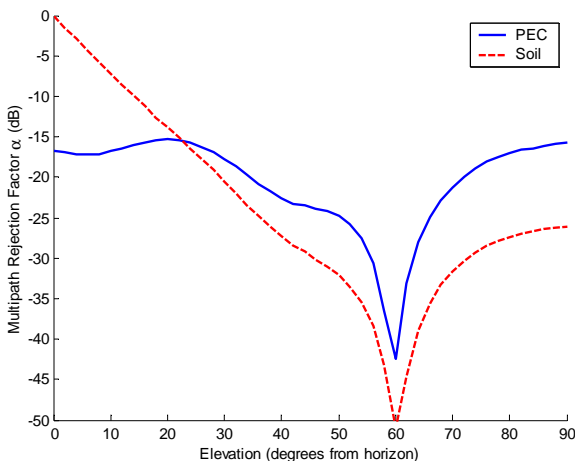


**Figure 5. Multipath rejection for the ARTUS antenna at L1**

shows the magnitude elevation patterns at the centre frequency of the Galileo E2-L1-E1 band (1575MHz). Using the single-ray multipath model, the multipath rejection factor  $\alpha$  was computed, using Equation (9), for a perfectly conducting ground and for a dielectric soil-like ground. The results are shown in Figure 5 for the same E2-L1-E1 band.

It is easy to see, by comparing the PEC result from Figure 5 and the radiation patterns in Figure 4 that the rejection factor is simply the difference between the right-hand CP gain and the left-hand CP gain at the corresponding ‘below horizon’ angle. It is harder to explain the behaviour for the soil-like dielectric, but essentially there are two differences:

- loss in the dielectric causes the reflected signal to be attenuated, so better rejection is achieved at high elevations (near zenith);
- the change of reflected wave from left- to right-handed elliptical/circular polarisation below the Brewster angle (about 28 degrees in this case) means that the antenna is no longer able to reject the multipath, by means of polarisation mismatch, because it too is right-hand CP at these angles. Hence  $\alpha$  tends to unity (0 dB) towards the horizon.

Numerical calculation of the carrier phase error  $\gamma$  using Equation (10), yields the results in Figure 6 below. The antenna height above the groundplane was set at 1m, so is reasonably typical of reference station installations. Note that the phase error has been converted to equivalent range error to make it more meaningful. As one might expect, the error due to multipath from the soil-like ground is generally much less than for PEC except at low elevation angles.

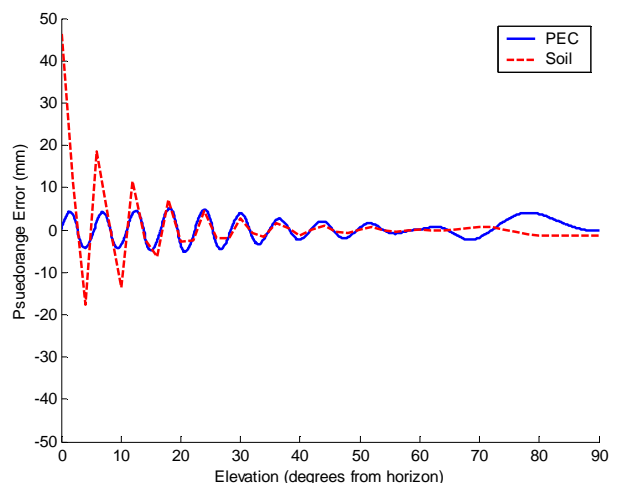


**Figure 6. Carrier phase error (as equivalent range error) for the ARTUS antenna at L1**

## GROUND SURFACE PROPERTIES

The examples in the last Section show the significance of the properties of the ground under the antenna, the complex relative permittivity  $\epsilon_r$  in particular. This parameter is a combination of the dielectric constant  $\kappa$ ; wavelength  $\lambda$  and the conductivity  $\sigma$ .

$$\epsilon_r \approx \kappa - j60\lambda\sigma$$

Some typical approximate values for dielectric constant and conductivity are given below for a variety of materials (at 20C, 1GHz). Many of these values are reproduced from graphs given in [4].

Description	Moisture Content (% vol)	$\kappa$	$\sigma$ ( $Sm^{-1}$ )
PEC	-	0	$\infty$
vacuum	-	1	0
pure water	-	~81	~0.3
salt water	-	~82	~5
clay	13	4.5	0.07
	76	50	0.8
	95	80	1.2
sand	0.5	3	n/a (very low)
	6	5	~0.015
	17	10	0.03
	37	25	0.08
silt	1.6	1.8	n/a (very low)
	68	50	0.27
	76	55	0.28
asphalt	n/a	3-5	n/a (low)
concrete	n/a	6-12	n/a (low)

**Table 1: Typical Values of Dielectric Constant and Conductivity for a Variety of Materials**

The conductivity of the ground has a profound effect on its reflectivity, and thus the magnitude of the multipath signal. In Figure 7, the solid blue and dashed red curves highlight the difference in multipath rejection possible between the two extremes of water/wet soil and dry sandy soil (6% water content). In fact, because the skin depth of water at these frequencies is very small (around 0.01mm), even surface wetness, such as after rainfall, might be sufficient to appear highly reflective. For very high precision applications (e.g. to within  $\pm 1mm$ ) such differences will be significant unless the antenna itself is naturally good at rejecting multipath.

## IMPROVING MULTIPATH REJECTION

It is clear that multipath from close-in reflecting surfaces can result in carrier phase errors at least as large as, if not somewhat larger than, any resulting from poor phase centre variation (PCV). Simulations have demonstrated

that, even for a reasonable antenna design, position errors of many millimetres can be expected. For most applications such errors are insignificant but for precision positioning, and especially the case of a reference station receiver, this is unacceptable. Fortunately, there are a number of techniques available for improving the multipath situation and these are discussed in the remainder of this section.

## Local Ground Plane

Most geodetic GNSS antennas are essentially planar, and usually incorporate some kind of ground plane (GP) or grounded cavity behind the element to direct gain in the forward (zenith) direction. If the element is shielded in this way, then for electromagnetic energy to find its way into the antenna from below (i.e. multipath) it must be as a result of diffraction around the perimeter of the GP. The key to controlling the backlobe then is to control this diffraction or to attenuate the approaching wave before it reaches the antenna.

Ideally, the GP would be infinitely large so that there is no edge to diffract around. A practical approximation to this might be to actually bury the antenna in the ground, so that it is flush with the surface, though this is likely to be inconvenient from the points of view of mechanical mounting, access, accumulation of dust, snow and other debris, and so on. Ideally, the conductivity of the ground nearby would also need to be guaranteed by surrounding the antenna by a large metallic plate or mesh.

A more practical alternative, especially if the antenna must be pillar-mounted, is to use a metallic plate alone. The work presented by Tatarnikov [3] suggests that the multipath rejection at elevation angles near zenith increases as the GP diameter is increased, but low-elevation performance worsens. Thus, an optimum is

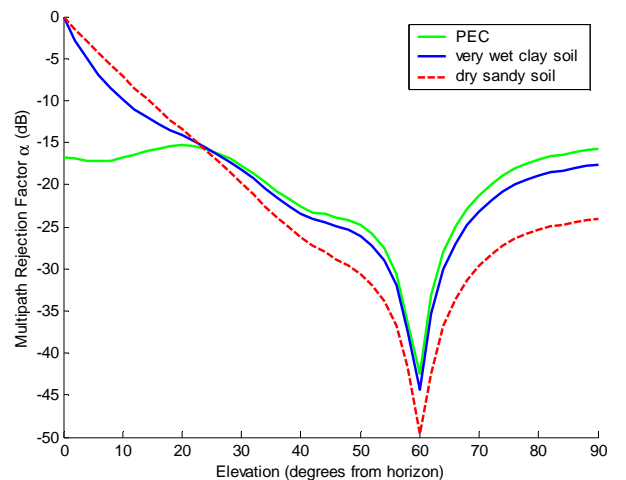


**Figure 7. The Effects of Ground Moisture Content on Multipath Rejection of the ARTUS Antenna at L1**

found for GPs that are approximately  $0.6\lambda$  in diameter. At the lowest frequency in the GNSS bands, this corresponds to about 150mm.

### Choke Rings

The most common approach to multipath mitigation is the use of a ‘choke ring ground plane’, which can be thought of as a very thick conductive ground plane with a number of deep, concentric grooves. Each groove is approximately  $\lambda/4$  deep and effectively forms a shorted transmission line due to the conductive walls. The short circuit impedance is transformed by the quarter-wave distance to an open circuit, so a high impedance is presented at the upper surface of the choke ring GP. This means that surface waves propagating across the GP decay at a faster rate (a “ $3/2$  power law”) than for a conventional flat ground plane (a “ $1/2$  power law”) and thus there is better multipath rejection. An alternative explanation for the mechanism by which choke ring GPs operate is given in [5]. A rigorous mathematical approach to modelling and predicting choke ring performance can be found in [7].

Whilst choke ring GPs provide superior performance over a flat GP, they are often larger in diameter and usually heavy and difficult to manufacture. Also, because of the resonant nature of the grooves, bandwidth is often very limited. Various techniques have been proposed to extend bandwidth, such as varying the groove depth from one ring to the next [9] and placing a frequency-selective surface (FSS) part-way down the groove to make it appear a different depth at different frequencies [5]. Other variations on the choke ring design include a “3D choke ring” [8] where the rings are stacked in a pyramid-like structure, or the “vertical choke ring” design [6] where rings are co-planar rather than concentric and are formed from circular plates.

### Lossy Ground Plane

Preventing electromagnetic scattering from sharp conducting edges has long been a goal of Stealth Engineers concerned with the reduction of the radar cross-section of ships and aircraft. A popular solution is the use of R-card: a non-conducting substrate coated with a resistive film, often where the sheet resistivity varies as a function of position from highly conducting to the impedance of free space. In this way, a sharp edge can be ‘blurred’ at high frequencies and the associated diffraction reduced. The same technique is employed by Trimble [10] in their patented ‘Stealth’ model ground planes, and has the significant advantage of wide bandwidth.

Rolled edges are also common, but the relatively low frequencies used for GNSS lead to very large dimensions.

### Local EBG Surface

An alternative method for producing high-impedance surfaces is the rapidly-growing field of Electromagnetic Band-Gap (EBG) structures, also variously referred to (sometimes incorrectly) as Photonic Band-Gap (PBG), Artificial Magnetic Conductor (AMC) and related to the Frequency Selective Surface (FSS). Essentially a regular, spatially-distributed network of capacitances and inductances can be made to exhibit unnatural electric and magnetic properties over a narrow range of frequencies. The most promising of these structures seems to be the planar “Sievenpiper” AMC [13], which consists of an array of metallic patches on the top surface of a dielectric sheet connected to a groundplane underneath by an array of vias. Its popularity has grown because it is possible to manufacture the structure using traditional printed circuit technology. The vias are carefully dimensioned to produce a certain inductance, whilst the gaps between the patches are capacitive. At or near the designed frequency, the surface simultaneously exhibits a high impedance to surface waves and also an approximately zero degree phase shift upon reflection of waves at normal incidence. This behaviour is characteristic of a perfect magnetic conductor, so is termed Artificial Magnetic Conductor (AMC).

The approach has been attempted as an alternative to the choke ring GP with some success (see [11] and [12]) but suffers two major flaws:

- the AMC ‘effect’ is limited to a relatively narrow band, making such structures difficult to apply to wideband, multi-GNSS antennas
- the large effective capacitances and inductances required for frequencies as low as 1.1 to 1.6GHz are difficult to implement in printed metallic structures on PCBs.

Whilst the latter may be solved by the use of printed spiral inductors and interdigitated capacitors, or even by chip components soldered to the board, the problem of bandwidth may be difficult enough to completely rule out the use of EBGs for multi-GNSS applications. In addition, the relatively large printed patterns required may also distort the antenna’s pattern making the phase centre less stable.

### Vertical (Array) Structures

Generally, the radiation pattern of an antenna can be controlled, including reduction of the backlobe, by introducing parasitic (electrically unconnected) or active (electrically connected) elements above and/or below the fed element, thus making a vertical array.

This approach has been tried with apparent success ([3], [14] and [15]) albeit at the expense of a more complicated and larger/taller antenna. The Integrated Multipath Limiting Antenna of [15] in particular easily meets a

specification of 30-35dB of rejection from 5° to zenith, but only for GPS L1. One potential concern is that arrays with many elements are likely to result in a gain pattern (in the upward direction) which has significant ripples or lobes. The side effect of this is an unstable phase centre, so whilst the multipath error may be small the phase centre error might well end up worse.

### Polarisation Rejection

Earlier in this paper the concept of *polarisation efficiency* was introduced. This is the idea that maximum power will be received when the antenna's polarisation characteristic matches that of the incident wave. The converse is also true, meaning that if we wish to reject a particular polarisation we must make an antenna with the following polarisation properties:

- same axial ratio
- opposite chirality (handedness or direction)
- orthogonally-aligned ellipse axes

In the example of Figure 1, at low elevation angles the multipath wave is right-hand elliptically polarised where the major axis of the ellipse is aligned horizontally. Thus, for maximum rejection, the antenna must exhibit a response at this elevation which has the *same* axial ratio, but which is *left-hand* elliptically polarised and with the major axis aligned *vertically*. In practice, it is difficult to control an antenna's polarisation except in the main lobe so this approach is highly impractical for single element antennas.

### Height Above Ground

Inspection of Equations (8a) or (8b) indicate that it is possible to reduce the phase error simply by reducing the path length difference between direct and reflected rays. One way to do this is to place the antenna on or very near to the ground surface. Even if this approach does not eliminate the error completely, it might be sufficiently independent of elevation angle to appear as an almost constant offset which is easily included in calibrations.

Alternatively, one would expect intuitively that placing the antenna very far away from the ground (i.e. high above it) should also reduce the effects of multipath. This is often true, although the reasons why are not obvious. If the ground is assumed to be a smooth, flat, infinite plane of homogeneous dielectric illuminated by a plane-wave, then the reflected wave is also a plane-wave and, as such, does not suffer spherical spreading (i.e.  $1/r^2$  decay in power with distance). No matter how high up the antenna is placed, the magnitude of the reflected wave, and therefore its influence, is the same. Of course, in reality the wave is not a plane wave but the satellites are so far away that the spreading is insignificant: a difference of 100m in antenna height results in a decrease in multipath power of a tiny fraction of one milli-dB, according to the

Friis Transmission Equation. Clearly the 'plane wave' assumption is not the one at fault.

Rough surfaces, on the other hand, scatter energy in a diffuse manner so that *many* contributions scattered from a *large* area of the ground will arrive at the antenna with almost *random* phases. The larger the reflection region, the greater the overall power contained in the sum of all these contributions, so one might think the multipath signal would grow. However, the path length difference between the contributions also grows, so the phases of the various contributions tend to occupy the whole range  $-pi$  to  $+pi$  and therefore cancel each other on average leading to lower multipath. The size of the reflection region is determined by the surface roughness, and the height of the antenna above the ground.

The assumption that real ground surfaces should be considered to be rough can be validated as follows. It is well known (from [16]) that the radiance of the specular component of the reflection appears to suffer attenuation when the surface is rough, approximately according to the following equation:

$$\rho \approx Fe^{-C^2}$$

where

$$C = \frac{4\pi \cdot \Delta h \cdot \sin \theta}{\lambda}$$

and  $F$  is the Fresnel coefficient of reflectance,  $\Delta h$  is the variation in surface height (roughness),  $\lambda$  is the wavelength and  $\theta$  is the grazing (elevation) angle. A surface might be considered smooth if the reflection is >95% specular, and <5% diffuse, for example. This corresponds to values of  $C$  of about 0.23 or less. Table 2 shows the maximum surface roughness values which meet this criterion:

	GPS L1 (1575MHz)	GPS L2 (1228MHz)
<i>zenith</i>	3.5mm	4.5mm
<i>45° above horizon</i>	4.9mm	6.3mm
<i>10° above horizon</i>	20mm	26mm

**Table 2: Values of surface height deviation corresponding to a 95% specular, 5% diffuse surface**

In fact, if the surface is non-conducting (i.e. dielectric) and not perfectly homogeneous, sub-surface scattering also occurs making the surface appear rougher.

For an incidence angle of 10° above the horizon, and an antenna 1m above the ground, the region of ground of interest can easily extend many metres in all directions. It is reasonable to assume that in real life surface deviations over this region are likely to be larger than just a few millimetres in practice, unless the ground has been

carefully prepared, and thus the surface should be considered rough.

### Modified Ground Surface

The possibility of treating the ground surface in some way is often overlooked as a means of reducing multipath errors. Clearly this is inconvenient for mobile applications, but much better suited to fixed reference stations – the focus of this paper. Such treatments might include one or more of the following:

- non-conducting / lossy surface (kept dry!)
- absorber material (e.g. RAM)
- deliberately roughened surface to increase diffuse scattering
- EBG surface to modify phase of reflected wave to be the same as the incident wave
- EBG surface to modify polarisation of reflected wave to exactly oppose that of the antenna (and therefore be rejected)
- a carefully-shaped reflector to scatter incident energy away from the antenna.

Such techniques might make good candidates for further research if the inconvenience of modifying many square metres of the ground was deemed worthwhile compared to, say, the convenience of a choke ring groundplane.

### Carrier Phase Error Correction

Equation (10) represents a method of determining the carrier phase error given the antenna's far-field gain, phase patterns and its height above a PEC groundplane. It should be possible to use this method to correct for the phase error in the receiver in much the same way that phase-centre variation (PCV) is corrected. In fact, such corrections could even be incorporated into the same 'ANTEX' format file as the PCV data, and treat both errors as one.

To make this approach practical, the antenna should be mounted as low as possible to the ground for two reasons:

- the carrier phase error is relatively slow-

changing with elevation angle, reducing the number of entries in the corrections file so that it is sampled every, say, 10 degrees.

- the area of ground required to be 'PEC-like' (i.e. a good conductor) is minimised to perhaps the order of a metre radius or so making it easier to control.

Once again, though, the constraints on how and where the antenna is mounted might be deemed unacceptably inconvenient compared to an antenna/groundplane with inherently good multipath rejection.

### A NOVEL GROUNDPLANE STRUCTURE

The methods of reducing multipath described so far fall into three broad categories:

1. try to stop the multipath from being produced (e.g. treat the ground itself with RAM, place the antenna on the ground or very high above it, etc.)
2. stop the multipath from diffracting around the edge of the antenna's local groundplane (e.g. the 'Stealth' or lossy groundplane, or no groundplane at all in the case of the vertical arrays)
3. stop the surface wave that arises from diffraction from reaching the antenna by presenting a high impedance (e.g. choke rings, AMC, etc.)

We considered an alternative to option 3: to stop the surface wave by reflecting it away from the antenna. The solution, illustrated in Figure 8, is a stretched 'C' shape formed by a large lower plane, a smaller upper plane and a vertical 'wall' separating the two. All three features are metallic, and must be axially symmetric (discs and cylinders) to ensure a stable phase centre.

The basic principle is as follows: the multipath wave diffracts around the leading edge of the lower

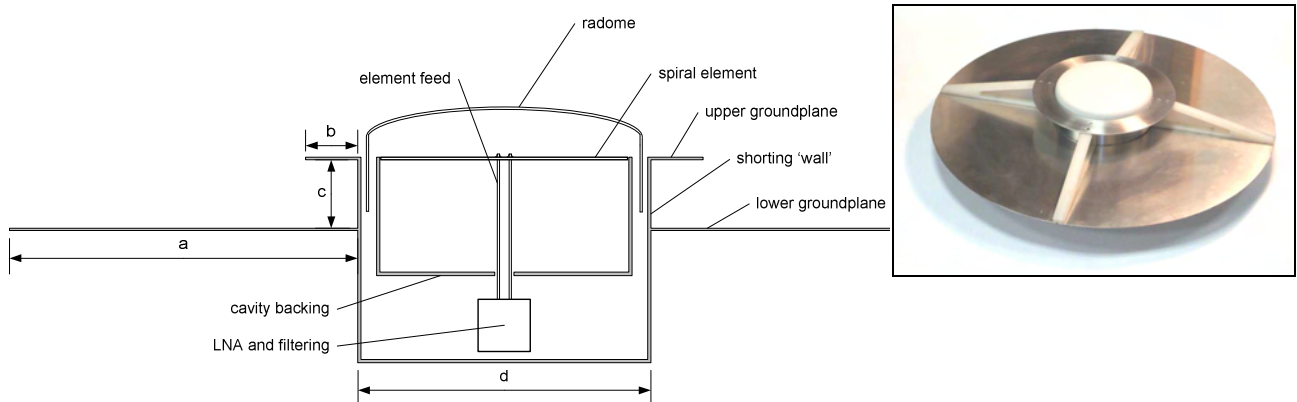
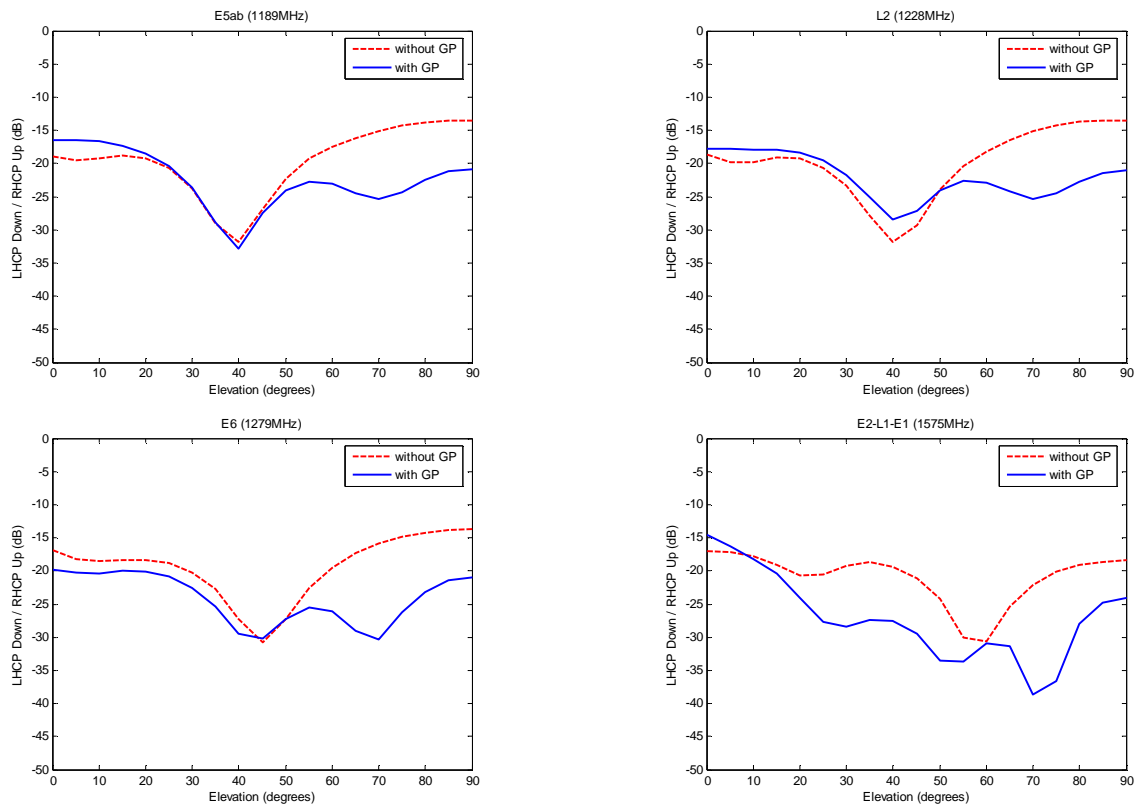


Figure 8. Cross-section diagram of the new groundplane and ARTUS antenna *in situ* (inset: photograph of prototype)



**Figure 9. Measured effects of the groundplane on the ARTUS antenna**

groundplane creating a vertically-polarised surface wave. The surface wave propagates towards the antenna until it encounters the upper groundplane. Together with the lower sheet, this forms a kind of parallel-plate waveguide which continues to guide the wave towards the antenna. Finally, the wave meets the ‘wall’ formed by the centre cylinder and is reflected back the way it came. It is likely that there is a secondary diffraction from the upper groundplane, but simulations show it to be relatively insignificant.

A number of candidate designs were simulated using Ansoft HFSS v11. To minimise the number of tetrahedra in the model, a crossed-dipole element was chosen instead of the spiral – it has a broadly similar radiation pattern but a much simpler geometry. The most-promising design was further optimised to maximise the ratio of RHCP gain ‘upwards’ to LHCP gain ‘downwards’. The resulting antenna and groundplane combination actually has a worse elevation phase centre stability than the antenna alone but this can be corrected for in the receiver and is justified by the improvement in multipath rejection. It is worth noting that the performance of this groundplane is shown in simulations to be significantly better than a simple metal disc of the same overall size.

The dimensions of the optimised solution are  $a = 180\text{mm}$ ,  $b = 30\text{mm}$ ,  $c = 40\text{mm}$ ,  $d = 152\text{mm}$ . Note that diameter  $d$

was chosen to accommodate the complete ARTUS antenna *inside* the structure including the radome – there is no electrical connection between antenna and groundplane but this has no noticeable effect on performance. A prototype based on these dimensions was constructed from aluminium and measured in Roke’s anechoic chamber; the results are given in Figure 9.

## CONCLUSIONS

Multipath from the ground beneath the antenna can have a critical impact on the positioning accuracy of a GNSS receiver, especially where centimetre or millimetre performance is desirable.

It is feasible that carrier phase errors that arise from such multipath can be corrected, but only with a good knowledge and/or control of the ground surface properties such as permittivity, moisture content (conductivity) and roughness. In practice it is more convenient to provide a local groundplane instead, but with the added problem of controlling diffraction from the edges at all frequencies of interest. In the future, it is expected that precision applications will require multiple GNSS corrections at many different frequencies pushing the limits of what is possible with ‘narrowband’ groundplane technologies like choke rings.

A possible groundplane solution is presented which is not dependent on resonant structures and is therefore inherently broad band. Measurements of a prototype show that, in conjunction with the ARTUS wideband spiral antenna, multipath rejection between 15 and 40dB is possible at all GPS and Galileo frequencies.

## ACKNOWLEDGMENTS

The authors acknowledge the support of the European GNSS Supervisory Authority (formerly Galileo Joint Undertaking), Area 1B "Technological Development" which, as one of their initiatives, has entered into contract for the development of advanced receiver technology for Galileo called "Advanced Receiver Terminal for User Services" (ARTUS).

## REFERENCES

- [1] R. Granger, P. Readman, S. Simpson, "The Development of a Professional Antenna for Galileo", Proceedings of ION GNSS September 2006.
- [2] P. Beckmann, "The depolarization of Electromagnetic Waves", The Golem Press, 1968.
- [3] D. Tatarnikov, V. Filippov, I. Soutiaguine, A. Astakhov, A. Stepanenko, P. Shamatulsky, "Multipath mitigation by conventional antennas with ground planes and passive vertical structures", GPS Solutions, vol.9 no. 3, September 2005.
- [4] J. O. Curtis, C. A. Weiss Jr., J. B. Everett, "Effect of Soil Composition on Complex Dielectric Properties", US Army Corps of Engineers, Technical Report EL-95-34, December 1995.
- [5] V. Filippov, D. Tatarnikov, J. Ashjaee, A. Astakhov, I. Sutiagin, "The First Dual-Depth Dual-Frequency Choke Ring", Javad Positioning Systems, November 1998.
- [6] Yoonjae Lee, Suman Ganguly, Raj Mitra, "Tri-band (L1, L2, L5) GPS Antenna with Reduced Backlobes", Proceedings of ION, September 1998.
- [7] J. M. Tranquilla, J. P. Carr, H. M. Al-Rizzo, "Analysis of a Choke Ring Groundplane for Multipath Control in Global Positioning System (GPS) Applications", IEEE Trans. Ant. Prop., vol. 42 no. 7, July 1994.
- [8] W. Kunysz, "A Three Dimensional Choke Ring Ground Plane Antenna", Proceedings of ION, September 2003.
- [9] T. L. Blakney, D. D. Connell, B. J. Lambert, J. R. Lee, "Broad-Band Antenna Structure Having Frequency-Independent, Low-Loss Ground Plane", US Patent #4,608,572, Issued August 26, 1986.
- [10] E. Krantz, P. Large, S. Riley, "GPS Antenna Design and Performance Advancements: The Trimble Zephyr", Trimble Navigation Limited white paper, 2001.
- [11] W. E. McKinzie III, R. B. Hurtado, B. K. Klimczak, J. D. Dutton, "Mitigation of Multipath Through the Use of an Artificial Magnetic Conductor for Precision GPS Surveying Antennas", IEEE Ant. and Prop. Soc. Intl. Symp., vol. 4, 2002.
- [12] P. de Maagt, R. Gonzalo, Y. Vardaxoglou, J-M. Baracco, "Electromagnetic Bandgap Antennas and Components for Microwave and (Sub)Millimeter Wave Applications", IEEE Trans. Ant. Prop., vol. 51 no.10, October 2003.
- [13] D. Sievenpiper, L. Zhang, R. F. J. Broas, N. G. Alexopolous, E. Yablonovitch, "High-impedance high-impedance electromagnetic surfaces with a forbidden frequency band," IEEE Trans. Microwave Theory Tech., vol. 47, pp. 2059–2075, November 1999.
- [14] C. C. Counselman III, "Multipath-Rejecting GPS Antennas", IEEE Proc., vol. 87 no.1, January 1999.
- [15] D. B. Thornberg, D. S. Thornberg, M. F. DiBenedetto, M. S. Braasch, F. van Graas, C. Bartone, "LASS Integrated Multipath-Limiting Antenna", NAVIGATION: Jnl. ION, vol. 50 no.2, summer 2003.
- [16] H. Davies, "The Reflection of Electromagnetic Waves from a Rough Surface", Proc. IEE 101, pp209-214, 1954.
- [17] R. C. Jones, "New calculus for the treatment of optical systems," J. Opt. Soc. Am. 31, pp488–493, 1941.